

## Widths of analog states in heavy elements from $(p, n)$ spectra\*

H. W. Fielding,<sup>†</sup> S. D. Schery, D. A. Lind, and C. D. Zafiratos  
*Nuclear Physics Laboratory, Department of Physics and Astrophysics, University of Colorado,  
 Boulder, Colorado 80302*

C. D. Goodman  
*Oak Ridge National Laboratory, Oak Ridge, Tennessee 37830*  
 (Received 17 December 1973; revised manuscript received 8 July 1974)

The  $(p, n)$  reaction on targets of  $^{197}\text{Au}$ ,  $^{206}\text{Pb}$ ,  $^{207}\text{Pb}$ ,  $^{208}\text{Pb}$ ,  $^{209}\text{Bi}$ , and  $^{232}\text{Th}$  has been studied to obtain the widths, reaction  $Q$  values, and selected cross sections of the isobaric analog of the ground state of these targets. Widths obtained are, respectively,  $116 \pm 35$ ,  $175 \pm 25$ ,  $192 \pm 25$ ,  $235 \pm 35$ ,  $257 \pm 35$ , and  $273 \pm 30$  keV assuming a Breit-Wigner line shape for the analog resonance. These results support the disagreement of previous  $(p, n)$  measurements with  $(p, n\bar{p})$  measurements for the widths of  $^{208}\text{Pb}$  and  $^{209}\text{Bi}$ . Results are shown to be sensitive to choice of resonance line shape and provide a possible explanation for discrepancies between  $(p, n)$  and  $(p, n\bar{p})$  measurements. The need for a more precise theoretical understanding of the structure of unbound analog resonances is indicated.

[NUCLEAR REACTIONS  $^{197}\text{Au}$ ,  $^{206, 207, 208}\text{Pb}$ ,  $^{209}\text{Bi}$ ,  $^{232}\text{Th}(p, n)$   $E = 25.8$  MeV measured widths of isobaric analog states.]

A discrepancy between the widths of isobaric analog states (IAS) in heavy nuclei as obtained by  $(p, n\bar{p})$ <sup>1,2</sup> and  $(p, p')$  resonance experiments<sup>3,4</sup> led to a measurement of the widths by the  $(p, n)$  reaction directly.<sup>5</sup> Likewise, measurements of the partial cross section for the  $(p, n)$  reaction to the analog states for targets of  $^{209}\text{Bi}$ ,  $^{197}\text{Au}$ , and  $^{181}\text{Ta}$  as obtained from  $\bar{p}$  measurements<sup>6</sup> led Grimes *et al.*<sup>7</sup> to measurements of the reaction cross section by observation of neutrons alone. Grimes *et al.* found a discrepancy with the  $\bar{p}$  measurements and presented a possible explanation in terms of several  $\bar{p}$  proton groups of almost identical energy.<sup>7</sup>

In this comment we present the results for width, reaction  $Q$  value, and selected cross section measurements for  $(p, n)$  studies of the isobaric analog of the ground state of the targets  $^{197}\text{Au}$ ,  $^{206}\text{Pb}$ ,  $^{207}\text{Pb}$ ,  $^{208}\text{Pb}$ ,  $^{209}\text{Bi}$ , and  $^{232}\text{Th}$  which are part of a systematic investigation of the  $(p, n)$  reaction over the whole mass range. These results, while differing in some specific cases, support the general disagreement between  $(p, n)$  and  $(p, n\bar{p})$  measurements for the widths and cross sections of the isobaric analog state, if a Breit-Wigner line shape is assumed for the resonance. We show that both cross sections and width measurements are sensitive to choice of line shape for the analog resonance and background, and that greater understanding of the resonance structure of unbound analog states is needed for more precise determinations of the widths and intensities of the analog resonances.

The experiment was performed on the University of Colorado rotating beam neutron time-of-flight spectrometer using 25.8 MeV protons and a flight path of 9.5 m. The cyclotron beam was gated by a grid at the ion source to transmit one pulse in six in order to prevent overlap of neutron spectra. The detectors consisted of 20 cm diam by 2.54 cm thick cells of NE 224 scintillator liquid, operated with usual  $n, \gamma$  discrimination techniques, and typical resolution in neutron time-of-flight spectra was 1.1 ns.

In order to remove the instrumental effects present in the width measurements, runs with  $^{12}\text{C}$  targets having the same energy loss as the target foils were interspersed among the heavy nuclei target runs. All targets used had energy losses between 20 and 30 keV. The  $^{12}\text{C}(p, n)^{12}\text{N}$  reaction has a similar  $Q$  value to the reactions being considered and since the natural width of the ground state of  $^{12}\text{N}$  is negligible, its width gave the instrumental resolution, which was about 100 keV and represents contributions from beam energy spread, target energy loss, timing spread, and kinematic spread. The kinematic spread was small even for the carbon target because the angles used were in the range from  $10^\circ$  to  $26^\circ$ . The  $\gamma$ -ray feed-through peaks were used to check for any time drift occurring between runs. Figure 1 shows a  $^{207}\text{Pb}$  spectrum with a  $^{12}\text{C}$  spectrum displayed to show the close proximity of the two reaction peaks and the location of feed-through  $\gamma$  rays. Spectra for the other targets (except  $^{232}\text{Th}$ ) are comparable. The intensity of the back-

ground of continuum neutrons from the target is in the range of 5 to 11 times the uniform target out background. In  $^{232}\text{Th}$  the IAS peak is broader in the time spectrum and further to the left (lower energy) due to the larger  $Q$  value for the reaction. The  $^{232}\text{Th}$  peak is located in a region of the neutron spectrum where the background is less linear and this made background determination more difficult.

The peak shape and background choice are major factors which enter into determining the natural width and cross section of the analog state and proved to be a source of major difficulty in analysis of the data. The upper three spectra in Fig. 2 show the result of least squares searches with a Gaussian line shape, Breit-Wigner line shape, and folded Gaussian plus Breit-Wigner line shape to the same data for the analog resonance of  $^{208}\text{Pb}$ . A linear background was assumed in each case and one channel corresponds to approximately 25 keV. Width values refer to full width at half-maximum. For the third spectrum, the Gaussian function which was folded with the Breit-Wigner line shape was fixed at a width of four channels to represent the instrumental resolution, and the search was conducted on the parameters of the Breit-Wigner function to give the folded result shown. For the three cases shown there is good agreement in the location of the peaks, but there is some discrepancy in the peak widths and major disagreement in the area under the Gaussian and Breit-Wigner line shapes. Unfortunately, the  $\chi^2$  per degree of freedom ( $\chi^2/\nu$ ), the statistical measure of the quality of agreement of line shape to data, is comparable in all cases and does not provide a guide for selection. Analysis of five

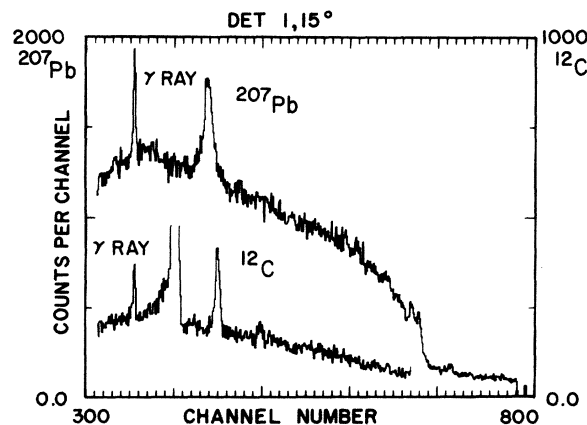


FIG. 1. A neutron time-of-flight spectrum for the  $(p, n)$  reaction on  $^{207}\text{Pb}$  at 25.8 MeV is shown as the upper curve. Below is superimposed a spectrum for a  $^{12}\text{C}$  target of comparable energy loss.  $\gamma$  ray feed-through peaks are shown as well as two neutron groups corresponding to the ground state and first excited state of  $^{12}\text{N}$ .

other spectra for  $^{208}\text{Pb}$  supported these comparisons of the Gaussian and Breit-Wigner line shapes. The width of the Gaussian line shapes had an average value of 1.05 times the Breit-Wigner line shapes while the area of the Gaussian line shapes was on the average 0.61 times the area of the

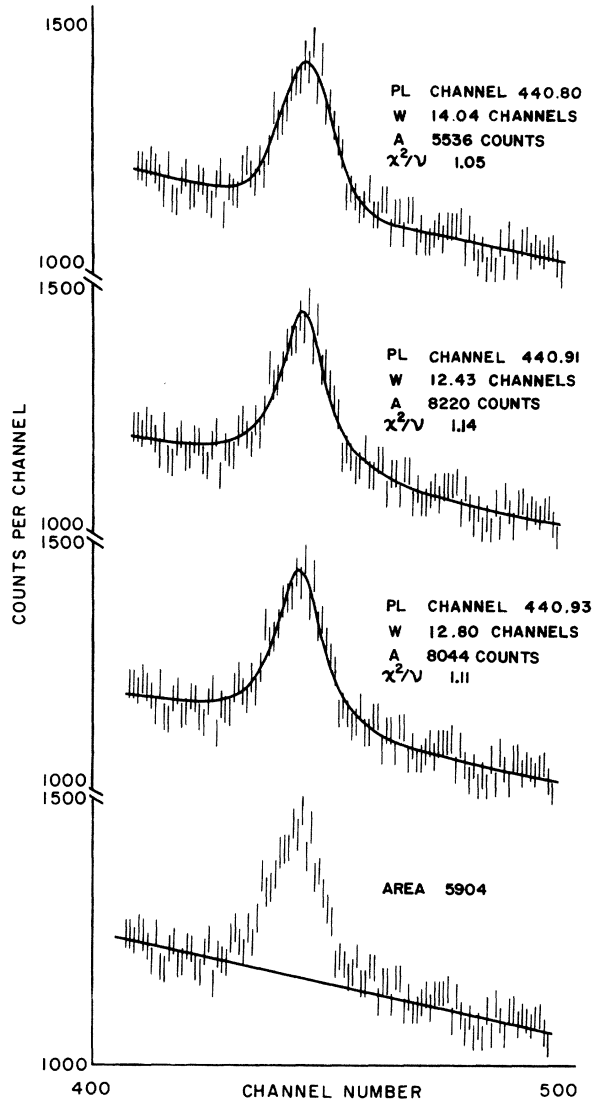


FIG. 2. The results of different procedures used to fit the same neutron time-of-flight data for the  $^{208}\text{Pb}$  IAS. For the upper three spectra, Gaussian, Breit-Wigner, and folded Gaussian plus Breit-Wigner line shapes were used, respectively, top to bottom. At the upper right of each spectrum, the peak location (PL), width (W), area (A), and  $\chi^2/\nu$  are indicated for the computer search. A change of one channel corresponds approximately to 25 keV and a linear background was assumed in each case. The area in the bottom spectrum was determined by visually adjusting a linear background to the data and summing counts above that background. The vertical bars are centered about the experimental data and have a length equal to twice the standard deviation.

TABLE I. Widths and  $Q$  values for isobaric analog states.

Isotope (parent)	$(p, n)$	$(p, n)^a$	$(p, n\bar{p})^a$	$(p, n)$ Breit-Wigner	$(p, n)$ Gaussian	$(p, n)^a$	$(p, n\bar{p})^a$	$(p, p')^a$
$^{197}\text{Au}$	$-18.555 \pm 0.020$			$116 \pm 35$	$158 \pm 35$			
$^{208}\text{Pb}$	$-18.944 \pm 0.020$	$-18.911 \pm 0.034$	$-18.899 \pm 0.024$	$175 \pm 25$	$220 \pm 25$	$196 \pm 26$	$230 \pm 38$	
$^{207}\text{Pb}$	$-18.919 \pm 0.020$	$-18.888 \pm 0.034$	$-18.875 \pm 0.028$	$192 \pm 25$	$236 \pm 25$	$203 \pm 32$	$540$	$170$
$^{208}\text{Pb}$	$-18.850 \pm 0.020$	$-18.831 \pm 0.020$	$-18.816 \pm 0.013$	$235 \pm 35$	$277 \pm 35$	$202 \pm 34$	$317 \pm 24$	$220 \pm 20$
$^{209}\text{Bi}$	$-19.030 \pm 0.025$	$-19.011 \pm 0.021$	$-18.991 \pm 0.012$	$257 \pm 35$	$299 \pm 35$	$151 \pm 34$	$327 \pm 31$	
$^{232}\text{Th}$	$-19.846 \pm 0.025$			$273 \pm 30$	$315 \pm 30$			

<sup>a</sup> Results in these columns taken from Ref. 5.

Breit-Wigner line shapes. Analysis of other spectra including those for other heavy nuclides resulted in the following observations. Results were not sensitive to choice of parabolic or linear background but it was important to choose a region of sufficient extent, as shown in Fig 2. Instrumental resolution could be represented well by a Gaussian line shape and was small enough that it was found unnecessary to modify the Breit-Wigner line shape for searches to the data which assumed the analog state was a Breit-Wigner resonance, since the folded shape of Gaussian and Breit-Wigner functions had essentially a Breit-Wigner structure. Correction for instrumental resolution could then be made by unfolding a Gaussian function from the simple Breit-Wigner function that fit the data.

The difficult decision was whether to choose a Breit-Wigner, Gaussian, or other distribution for the intrinsic shape of the analog resonance. Although a simple Breit-Wigner distribution might seem the first choice, it is not in general true that this is the line shape of the analog resonances, particularly those which are unbound.<sup>8,9</sup> The only justification for a Gaussian distribution is perhaps simplicity (the Gaussian line shape provided agreement to data comparable to that obtained with a Breit-Wigner line shape as measured by values of  $\chi^2/\nu$ ) or the fact that if the analog resonance is composed of several partial distributions it is known that the sum of arbitrary statistical distributions sometimes approaches the Gaussian distribution as a limit.<sup>10</sup> There is the additional problem that the background under the analog peaks is predominantly caused by reactions in the target and not instrumental effects or secondary scattering and hence might coherently interfere with the analog resonance. Careful analysis of the spectra provided some insight into these questions but was not conclusive. The data were fitted with a peak shape given by the function

$$f(E) = \frac{0.25a_1a_2^2}{(E - a_3)^2 + a_4(E - a_3)^4 + 0.25a_2^2} \quad (1)$$

This function was chosen because it was a convenient parameterization which would indicate through the parameter  $a_4$  how the data behave compared to predictions with a Breit-Wigner function. Results indicated that the peak falls off faster than predicted by a Breit-Wigner function or a Breit-Wigner function folded with a narrow Gaussian function but not as fast as a Gaussian function alone. The use of function (1) did not change the peak width significantly from the result with a Breit-Wigner function but did reduce the peak area significantly. However, the results were not consistent enough to make more quantitative statements with this function. Therefore, it was decided to analyze the data using both Gaussian and Breit-Wigner line shapes.

Peak widths determined assuming a Breit-Wigner line shape for the analog resonance and a Gaussian line shape for the instrumental resolution are given in column 4 of Table I. The Gaussian contribution was unfolded using an approximation method described by McEwen.<sup>11</sup> The error in this method is much less than the errors quoted in column 4 which represent the spread in results obtained from independent determinations for each target. Column 5 of Table I lists the widths of the analog states assuming a Gaussian line shape for the analog resonance. The increase in width is caused chiefly by the smaller effect of unfolding a narrow Gaussian function from a Gaussian function compared to unfolding a narrow Gaussian function from a Breit-Wigner function.

Table II, column 2, shows the calculation for total cross sections for  $^{197}\text{Au}$ ,  $^{208}\text{Pb}$ , and  $^{209}\text{Bi}$ . To avoid questions of peak shape, the results were obtained by visually fitting a linear background to the spectra and totaling counts above the background. The bottom spectrum in Fig. 2 shows an area determined by this method. Errors quoted include effects of detector efficiency, target thickness, and repeatability of background choice as determined by independent observers but do not reflect systematic errors that might be present in the assumption of a limited peak width and

TABLE II.  $\sigma(p, n)$  and  $\sigma(p, n\bar{p})$  for  $^{197}\text{Au}$  and  $^{209}\text{Bi}$ .

Target	Bombarding energy (MeV)	$\sigma(p, n)^a$ (mb)	$\sigma(p, n)^b$ (mb)	$\sigma(p, n\bar{p})^c$ (mb)
$^{197}\text{Au}$	25.0		7.3	2.0
	25.8	$6.31 \pm 0.88$		
	27.0		6.8	2.0
$^{208}\text{Pb}$	25.8	$9.61 \pm 1.15$		
$^{209}\text{Bi}$	24.8			14.9
	25.0		5.4	
	25.8	$6.94 \pm 1.11$		
	26.1			14.5
	27.0		5.7	

<sup>a</sup> Cross section from Ref. 12.

<sup>b</sup> Cross section from Ref. 7.

<sup>c</sup>  $\bar{p}$  cross sections as compiled in Ref. 7.

linear background. Additional discussion of cross section calculations are discussed by Schery *et al.*<sup>12</sup> For comparison, an assumption of Gaussian line shape plus linear background would yield a result  $21 \pm 4\%$  smaller while an assumption of Breit-Wigner line shape plus linear background would yield a result  $33 \pm 6\%$  larger for the cross sections.

Reaction  $Q$ -value results are shown in column 1 of Table I. These results were insensitive to choice of line shape and the errors shown represent the spread in results obtained from independent measurements. Measurements of the  $^9\text{Be}(p, n)^9\text{B}$  and  $^{12}\text{C}(p, n)^{12}\text{N}$  reactions which have widely different  $Q$  values provided the calibration for the beam energy and time-of-flight spectrum.

The  $Q$ -value measurements reported in this paper are in good agreement with results tabulated by Crawley *et al.* in their paper<sup>5</sup> and shown in Table I as well as with those compiled by Jänecke.<sup>13</sup> Except for  $^{209}\text{Bi}$ , the analog widths determined with the Breit-Wigner line shape are in agreement with the  $(p, n)$  results obtained by the Michigan State University group<sup>5</sup> which were also obtained assuming a Breit-Wigner resonance and are listed in column 6 of Table I. Our results also agree with the measurements by  $(p, p')$  experiments for  $^{207}\text{Pb}$  and  $^{208}\text{Pb}$  shown in column 8 but are significantly smaller than the  $(p, n\bar{p})$  results for  $^{207}\text{Pb}$  and  $^{208}\text{Pb}$  listed in column 7 of Table I. However, it is important to note that analysis of present

data with a Gaussian line shape increases the analog widths and would bring them into agreement with the  $(p, n\bar{p})$  results except for  $^{207}\text{Pb}$ , as can be seen by comparing columns 5 and 7.

Table II compares total  $(p, n)$  cross sections with those deduced from  $(p, n\bar{p})$  experiments. Our measurements agree with those of Grimes<sup>7</sup> shown in column 3 for  $^{197}\text{Au}$  and are only in modest disagreement for  $^{209}\text{Bi}$ . Even assuming a Gaussian line shape or Breit-Wigner line shape for the analog resonance our results would substantiate the disagreement with  $(p, n\bar{p})$  results shown in column 4. Grimes *et al.*<sup>7</sup> proposed an interpretation of this disagreement suggesting that several excited analog states of  $^{209}\text{Bi}$  in  $^{209}\text{Po}$  decaying by proton emission with the same energy would account for the large  $\bar{p}$  cross section. However, if this were true, neutron groups of appropriate energy should occur in the  $(p, n)$  measurements over about 3 MeV range below the analog state group with a net intensity as large as that of the ground state group. No evidence for such an anomalous cross section has appeared in our runs. Observations on a wide variety of nuclear targets have shown that excitation of excited analog states falls off strongly with mass number beyond  $A = 90$ .

Present measurements of both widths and cross sections tend to support the disagreement of  $(p, n)$  results with  $(p, n\bar{p})$  results. However, the explanation proposed by Grimes *et al.*<sup>7</sup> is difficult to accept unless experimental evidence for the population of excited analog states is found. An alternate explanation might be that the discrepancy is due entirely to difficulties with experimental precision and reduction of the data. Our analysis indicates that it is possible to obtain comparable agreement to  $(p, n)$  data as determined by  $\chi^2/\nu$  values with choices for resonance line shape and background which provide significantly different values for both peak area and width. Since experimental  $(p, n)$  spectra cannot simultaneously determine resonance shape and background structure uniquely, it seems important to have further theoretical insight into the structure of unbound isobaric analog resonances and the underlying neutron continuum before more careful comparisons of  $(p, n)$ ,  $(p, n\bar{p})$ , and  $(p, p')$  measurements can be made.

\*Work supported in part by the U. S. Atomic Energy Commission.

†Permanent address: Department of Physics, University of Wyoming, Laramie, Wyoming.

<sup>1</sup>G. M. Crawley and P. S. Miller, Phys. Rev. C **6**, 306

(1972).

<sup>2</sup>G. M. Crawley, W. Benenson, P. S. Miller, D. L. Bayer, R. St. Onge, and A. Kromminga, Phys. Rev. C **2**, 1071 (1970).

<sup>3</sup>C. D. Kavaloski, J. S. Lilley, P. Richard, and N. Stein,

- Phys. Rev. Lett. 16, 807 (1966); G. M. Temmer, G. H. Lenz, and G. T. Garvey, in *International Nuclear Physics Conference*, edited by R. L. Becker, C. D. Goodman, P. H. Stelson, and A. Zucker (Academic, New York, 1967), p. 255.
- <sup>4</sup>B. L. Anderson, J. B. Bondorf, and B. S. Madsen, Phys. Lett. 22, 651 (1966); G. H. Lenz and G. M. Temmer, Nucl. Phys. A112, 625 (1968); G. W. Bund and J. S. Blair, *ibid.* A144, 384 (1970).
- <sup>5</sup>G. M. Crawley, P. S. Miller, A. Galonsky, T. Amos, and R. Doering, Phys. Rev. C 6, 1890 (1972).
- <sup>6</sup>G. W. Hoffmann, W. H. Dunlop, G. J. Igo, J. G. Kulleck, J. W. Sunier, and C. A. Whitten, Jr., Nucl. Phys. A187, 577 (1972).
- <sup>7</sup>S. M. Grimes, J. D. Anderson, J. C. Davis, W. M. Dunlop, and C. Wong, Phys. Rev. Lett. 30, 992 (1973).
- <sup>8</sup>A. M. Lane, in *Isospin in Nuclear Physics*, edited by D. H. Wilkinson (North-Holland, Amsterdam, 1969), p. 547.
- <sup>9</sup>G. W. Bund and J. S. Blair, Nucl. Phys. A144, 384 (1970).
- <sup>10</sup>E. B. Wilson, *An Introduction to Scientific Research* (McGraw-Hill, New York, 1952), p. 246.
- <sup>11</sup>J. G. McEwen and G. J. Daniell, Nucl. Instrum. Methods 116, 169 (1974).
- <sup>12</sup>S. D. Schery, D. A. Lind, H. W. Fielding, and C. D. Zafiratos, unpublished.
- <sup>13</sup>J. Jänecke, in *Isospin in Nuclear Physics* (see Ref. 8), p. 297.